Data-Driven Model Predictive Control with Performance Constraint for Wastewater Treatment Processes

Yan Wang[1], Hao-Yuan Sun[1], Hong-Gui Han[*,1], Zheng Liu[1], Hao-Ran Mu[1]

1. School of Information Science and Technology, Beijing University of Technology, Beijing 100124, China
E-mail: rechardhan@sina.com

Abstract: Strict effluent quality standards and physical limitations of the equipment make accurately controlling dissolved oxygen (DO) concentration in wastewater treatment processes (WWTPs) a challenging task. In this paper, a data-driven model predictive control strategy with performance constraint (PC-MPC) is proposed to ensure accurate tracking of DO concentration set-point. First, a data-driven model is established using the fuzzy neural network, effectively addressing the problem of complex nonlinear modeling of WWTPs and providing accurate predictive output for the control process. Second, a model predictive control (MPC) strategy with performance constraint is designed, in which tracking error is considered as a performance constraint index within the MPC framework, enabling accurate tracking of the DO concentration to the desired set-point. Third, an adaptive constraint optimization algorithm based on the Levenberg-Marquardt (L-M) method is developed. By utilizing the exponential penalty function to reformulate the system constraints, the finite horizon optimization control problem can be directly solved to determine the optimal control sequence. Finally, the stability of the proposed PC-MPC strategy is proven through theoretical analysis and its effectiveness is validated on the benchmark simulation model No. 1.

Key Words: Model predictive control, fuzzy neural network, input and output constraints, wastewater treatment processes

1 Introduction

With the acceleration of urbanization, a high volume of domestic and industrial wastewater is discharged, which brings enormous pressure to the environment [1], [2]. The activated sludge method, as an efficient and economical biological wastewater treatment technology, is widely used in wastewater treatment processes (WWTPs) [3]. This technology degrades pollutants in water through the metabolic process of microorganisms, where dissolved oxygen (DO) is a necessary condition for microbial metabolism in the activated sludge process, and its concentration directly affects the activity and treatment efficiency of microorganisms [4], [5]. Low DO concentration may lead to weakened microbial metabolic activity and affect the degradation efficiency of pollutants. Excessive DO concentration may lead to energy waste and increased operating costs [6], [7]. Therefore, developing an intelligent control method to maintain the DO concentration within an appropriate range is of practical significance for improving treatment efficiency and ensuring the effluent quality of WWTPs.

Given the importance of controlling the DO concentration in the activated sludge WWTP, numerous control methods have been proposed to accurately regulate the DO concentration [8]. For example, Qiao *et al*. proposed a pipelined recurrent wavelet neural network (PRWNN) control method for controlling the DO concentration in WWTPs [9]. In this method, an online growth strategy was designed to automatically regulate the number of controller modules, and the controller structure was determined to adapt to different operating conditions. The simulation results showed that the PRWNN controller can improve the control accuracy. Stebel *et al*. introduced the idea of a boundary-based predictive controller (BBPC) for the laboratory activated sludge device with an ON-OFF actuator [10]. In this method, the dynamic parameters of the DO concentration model were identified and the adaptability was provided when the process load disturbance changes significantly. The experimental comparison with traditional controllers demonstrated the superiority of the proposed BBPC. The aforementioned controllers demonstrated remarkable control accuracy, enabling the DO concentration to be maintained within the desired range. However, while striving for efficient control, it is imperative to fully consider and address the constraints posed by the physical performance of the equipment to maintain the safety and stability of the system [11], [12].

Model predictive control (MPC) is a sophisticated approach that comprehensively considers system control objectives and constraints [13], [14]. By employing iterative optimization, the control sequence that satisfies the constraints and optimizes system performance can be obtained [15]. Xu *et al*. proposed a constrained model predictive direct speed control strategy for permanent magnet synchronous motor speed control [16]. This design reduced the computational burden by introducing the Laguerre function and achieved long-horizon MPC optimization with constraints. Yan *et al*. developed a stochastic MPC strategy for linear systems with disturbances [17]. This method utilized the Chebyshev inequality to handle the chance constraint of the sum of discounted violation probabilities over an infinite horizon. By dynamically adjusting feedback gains in real-time, the conservatism associated with constraint processing was reduced, thereby enhancing the control performance. The aforementioned methods exhibit certain innovation and effectiveness in handling system constraints. However, they rely on the exact system model, which poses challenges for their application in WWTPs. In order to provide accurate

[*]This work was supported by National Science Foundation of China under Grants 62125301, 62021003, 62303024, 62473011, and U24A20275, National Key Research and Development Project under Grants 2022YFB3305800-5, Beijing Nova Program under Grant K7058000202402, Youth Beijing Scholar under Grant No.037, and Science and Technology Special Projects of Xicheng District, Beijing under Grant XCSTS-TI2024-08. (Corresponding author: Hong-Gui Han).

predictive output for the control process and ensure the control accuracy of DO concentration, identifying the system model based on data-driven methods is a practical and feasible approach.

Based on the above analysis, a data-driven MPC strategy with performance constraint (PC-MPC) is developed to track the DO concentration to the desired set-point in WWTPs. The main contributions are outlined below.

1) A data-driven prediction model based on a fuzzy neural network (FNN) is established. The model parameters are corrected based on the prediction error to accurately identify the WWTP and provide precise predicted outputs for the control process.

2) A MPC strategy with performance constraint is designed. Apart from considering the physical limitation of the aeration equipment and the constraint on the DO concentration, the tracking error is also incorporated as a performance constraint within the MPC framework. This approach improves the accuracy of the system response, ensuring that control objectives are achieved more safely and effectively.

3) An constraint optimization algorithm based on the Levenberg-Marquardt (L-M) method is designed. By reformulating system constraints with the exponential penalty function, the finite horizon optimal control problem is reconstructed, which can be directly solved to determine the optimal control sequence.

2 Problem Formulation

The DO concentration of unit 5 (S_{O5}) in the biochemical reaction tank is the key variable affecting the treatment efficiency and effluent quality of the WWTP control system. The accurate tracking of S_{O5} to the set-point is achieved by modifying the oxygen transfer coefficient of the fifth unit (K_{La5}). The WWTP control system involves numerous complex biochemical reactions, exhibiting highly nonlinear, and uncertain dynamic characteristics. The system can be expressed as follows

$$y(k+1) = f(y(k), u(k)), \tag{1}$$

where $f(\cdot)$ represents the unknown nonlinear function, $y(k)$ represents the S_{O5} at time k, $u(k)$ represents the K_{La5} at time k.

To ensure the effective operation of the WWTP control system, the input and output constraints are set to

$$u_{\min} \le u(k) \le u_{\max}, \tag{2}$$

$$y_{\min} \le y(k) \le y_{\max}, \tag{3}$$

where $u_{\min}$ and $u_{\max}$ stand for the minimum and maximum values allowed for K_{La5}, $y_{\min}$ and $y_{\max}$ represent the minimum and maximum values of S_{O5}, respectively.

In addition, to ensure accurate regulation of S_{O5} to the predetermined range, optimize treatment efficiency, and avoid resource waste caused by excessive aeration, the tracking error of S_{O5} is constrained as follows

$$e_{\min} \le e(k) \le e_{\max}, \tag{4}$$

where $e(k)=y(k)-y_r(k)$, $y_r(k)$ is the set-point at time k, $e_{\min}$ and $e_{\max}$ stand for the minimum and maximum values allowed for the tracking error, respectively.

This paper aims to develop a data-driven MPC method for WWTP control systems with unknown dynamics to achieve accurate control of S_{O5} and satisfy constraints (2)-(4).

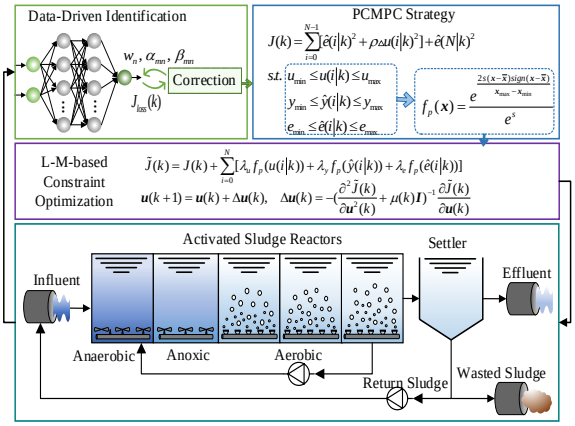

Fig. 1 The structure diagram of PC-MPC strategy.

3 Data-driven PC-MPC strategy

In this section, a PC-MPC method is developed to achieve accurate control of S_{O5}. As shown in Fig. 1, the PC-MPC strategy consists of three parts: data-driven system identification, PC-MPC framework formulation, and adaptive constraint optimization.

3.1 Data-Driven System Identification

FNN has the ability to deal with complex nonlinear relations and optimize internal parameters through continuous learning [18], a data-driven prediction model based on the FNN is established to learn the pattern from the operating data and realize the accurate identification of the WWTP control system with unknown dynamic and complex nonlinearity. The input vector of the FNN at time k is $\boldsymbol{x}(k)=[x_1(k), ..., x_q(k)]$, and the output of the FNN at time k is represented as

$$\hat{y}(k) = \sum_{n=1}^{p} w_n(k) v_n(k), \tag{5}$$

where $\hat{y}(k)$ represents the predicted S_{O5} at time k, p represents the number of neurons in the normalized layer, $w_n(t)$ represents the connection weight between the n-th normalized neuron and output neuron, $v_n(t)$ represents the output of the n-th normalized neuron, expressed as

$$v_n(k) = \frac{e^{-\sum_{m=1}^{q} \frac{(x_m(k)-\alpha_{mn}(k))^2}{2(\beta_{mn}(k))^2}}}{\sum_{j=1}^{p} e^{-\sum_{m=1}^{q} \frac{(x_m(k)-\alpha_{mj}(k))^2}{2(\beta_{mj}(k))^2}}}, \tag{6}$$

where $x_m(k)$ represents the m-th input, q represents the number of neurons in the input layer, $\boldsymbol{\alpha}_j(t)=[\alpha_{1j}(t), ..., \alpha_{qj}(t)]^{\mathrm{T}}$ and $\boldsymbol{\beta}_j(t)=[\beta_{1j}(t), ..., \beta_{qj}(t)]^{\mathrm{T}}$ stands for the center vector and width vector of the j-th RBF neuron, respectively.

To effectively train and optimize the FNN model, the loss function is set as

$$J_{loss}(k) = \frac{1}{2}(y(k) - \hat{y}(k))^2. \tag{7}$$

The gradient descent algorithm is used to update the weight, center, and width

$$w_n(k+1) = w_n(k) - \eta \frac{\partial J_{loss}(k)}{\partial w_n(k)}, \tag{8}$$

$$\alpha_{mn}(k+1)=\alpha_{mn}(k)-\eta\frac{\partial J_{loss}(k)}{\partial \alpha_{mn}(k)}, \tag{9}$$

$$\beta_{mn}(k+1)=\beta_{mn}(k)-\eta\frac{\partial J_{loss}(k)}{\partial \beta_{mn}(k)}, \tag{10}$$

where η is the learning rate.

The constructed prediction model is trained based on historical data and updated with gradient descent algorithm to ensure accurate prediction output during the control process. Then, based on the current system output $y(k)$ and future control input sequence $\boldsymbol{u}(k)=[u(0|k),\ u(1|k),\ ...,\ u(N\text{-}1|k)]^{\mathrm{T}}$, recursively calculate the system prediction output $\hat{\boldsymbol{y}}(k)=[\hat{y}(1|k),\ \hat{y}(2|k),\ ...,\ \hat{y}(N|k)]^{\mathrm{T}}$ within the prediction horizon N, the detailed process is as follows.

In the first step of prediction, the input vector of the FNN is $\boldsymbol{x}(k)=[y(k),\ u(0|k)]$, and the predicted output is $\hat{y}(1|k)$. In the second step of prediction, the input vector of the FNN is $\boldsymbol{x}(k)=[\hat{y}(1|k),\ u(1|k)]$, and the predicted output is $\hat{y}(2|k)$. The prediction output of the current step is taken as the input of the FNN for the next prediction to obtain the prediction output of the next step. Iterate this process until the N-th step predicted output $\hat{y}(N|k)$ is obtained.

3.2 PC-MPC Strategy

The PC-MPC strategy strives for accurate DO concentration tracking to the set-point while satisfying system constraints. To this end, the finite horizon optimization control problem (FHOCP) with system constraints is defined as

$$\min_{u} J(k)=\min_{u}\sum_{i=1}^{N}\hat{e}(i|k)^2+\rho\sum_{i=0}^{N-1}\Delta u(i|k)^2, \tag{11}$$

$$\text{s.t.}\quad \hat{y}(0|k)=y(k), \tag{12}$$

$$\hat{y}(i|k)=\sum_{n=1}^{p}w_n(k)v_n(i|k), \tag{13}$$

$$u_{\min}\le u(i|k)\le u_{\max}, \tag{14}$$

$$y_{\min}\le \hat{y}(i|k)\le y_{\max}, \tag{15}$$

$$e_{\min}\le \hat{e}(i|k)\le e_{\max}, \tag{16}$$

where $\hat{e}(i|k)=\hat{y}(i|k)\text{-}y_r(k+i)$ represents the i-step ahead tracking error at time k, $y_r(k+i)$ is the set-point at time $k+i$, $\Delta u(i|k)=u(i|k)\text{-}u(i|k\text{-}1)$ denotes the i-step ahead control input increment at time k, $u(i|k)$ is the i-step ahead control input at time k, $u(i|k\text{-}1)$ is the i-step ahead control input at time k-1, ρ represents the weight parameter, N is the planning horizon.

3.3 Adaptive Constraint Optimization

The existence of constraint conditions (14)-(16) limits the range of values for the output variable and the control variable, thereby affecting the value of the cost function (11). Usually, iterative algorithms are used to solve the FHOCP, which requires repeatedly calculating the objective function (11) and determining the constraints (14)-(16), consuming a large amount of computing resources. To address this problem, exponential penalty terms are constructed based on the characteristics of the constraint conditions and added to the cost function, thereby transforming the constrained optimization problem into an unconstrained optimization problem. Then, the L-M algorithm is utilized to minimize the cost function, obtaining the optimal solution that satisfies the constraints and has good performance.

For constraint (14), an exponential penalty function with a sharpness variable is designed as

$$f_p(u)=\frac{e^{\frac{2s_u(u-\bar{u})sign(u-\bar{u})}{u_{\max}-u_{\min}}}}{e^{s_u}}, \tag{17}$$

where variable s_u is the sharpness of the function $f_p(u)$, $\bar{u}=(u_{\min}+u_{\max})/2$, $sign(\cdot)$ represents a symbolic function,

$$sign(u-\bar{u})=\begin{cases}1, & u>\bar{u},\\ 0, & u=\bar{u},\\ -1, & u<\bar{u}.\end{cases} \tag{18}$$

The penalty term $f_p(u)$ remains constant when the predicted output $\hat{y}$ is between the bounds u_{min} and u_{max}, but it increases exponentially when the predicted output $\hat{y}$ is far from its bounds.

Similarly, for constraints (15)-(16), the exponential penalty terms are constructed as follows

$$f_p(\hat{y})=\frac{e^{\frac{2s_y(\hat{y}-\bar{y})sign(\hat{y}-\bar{y})}{y_{\max}-y_{\min}}}}{e^{s_y}}, \tag{19}$$

$$f_p(\hat{e})=\frac{e^{\frac{2s_e(\hat{e}-\bar{e})sign(\hat{e}-\bar{e})}{e_{\max}-e_{\min}}}}{e^{s_e}}, \tag{20}$$

where variables s_y and s_e are the sharpness of the function $f_p(\hat{y})$ and $f_p(\hat{e})$, $\bar{y}=(y_{\min}+y_{\max})/2$, $\bar{e}=(e_{\min}+e_{\max})/2$.

Then, the cost function $J(k)$ (11) is reconstructed as

$$\begin{aligned}\tilde{J}(k)=&\sum_{i=1}^{N}\hat{e}(i|k)^2+\rho\sum_{i=0}^{N-1}\Delta u(i|k)^2\\ &+\sum_{i=0}^{N-1}\lambda_u f_p(u(i|k))+\sum_{i=1}^{N}[\lambda_y f_p(\hat{y}(i|k))+\lambda_e f_p(\hat{e}(i|k))].\end{aligned} \tag{21}$$

The cost function (21) is minimized at time k to obtain the optimal control sequence using the L-M algorithm

$$\boldsymbol{u}(k)=\boldsymbol{u}(k-1)+\delta\Delta\boldsymbol{u}(k), \tag{22}$$

$$\Delta\boldsymbol{u}(k)=-\left(\frac{\partial^2\tilde{J}(k)}{\partial\boldsymbol{u}^2(k)}+\mu(k)\boldsymbol{I}\right)^{-1}\frac{\partial\tilde{J}(k)}{\partial\boldsymbol{u}(k)}, \tag{23}$$

where δ is the learning rate, $\partial\tilde{J}(k)/\partial\boldsymbol{u}(k)$ is the gradient of the cost function, $\partial^2\tilde{J}(k)/\partial\boldsymbol{u}^2(k)$ is the Hessian matrix, $\mu(k)$ is the regularization parameter, and $\boldsymbol{I}$ is the identity matrix. By the receding horizon principle, the MPC control law is determined from the first element of the optimal control sequence.

For the sake of presentation, the following definitions are provided

$$\hat{\boldsymbol{e}}(k)=[\hat{e}(1|k),\ \hat{e}(1|k),\ ...,\ \hat{e}(N|k)]^{\mathrm{T}}, \tag{24}$$

$$F_p(\boldsymbol{u}(k))=[f_p(u(0|k)),\ f_p(u(1|k)),\ ...,\ f_p(u(N-1|k))]^{\mathrm{T}}, \tag{25}$$

$$F_p(\hat{\boldsymbol{y}}(k))=[f_p(\hat{y}(1|k)),\ f_p(\hat{y}(1|k)),\ ...,\ f_p(\hat{y}(N|k))]^{\mathrm{T}}, \tag{26}$$

$$F_p(\hat{\boldsymbol{e}}(k))=[f_p(\hat{e}(1|k)),\ f_p(\hat{e}(1|k)),\ ...,\ f_p(\hat{e}(N|k))]^{\mathrm{T}}, \tag{27}$$

The gradient of the cost function (21) is calculated as

$$\begin{aligned}\frac{\partial\tilde{J}(k)}{\partial\boldsymbol{u}(k)}=&2\frac{\partial\hat{\boldsymbol{e}}^{\mathrm{T}}(k)}{\partial\boldsymbol{u}(k)}\hat{\boldsymbol{e}}(k)+2\rho\frac{\partial\Delta\boldsymbol{u}^{\mathrm{T}}(k)}{\partial\boldsymbol{u}(k)}\boldsymbol{u}(k)\\ &+\lambda_u\frac{\partial F_p(\boldsymbol{u}(k))}{\partial\boldsymbol{u}(k)}+\lambda_y\frac{\partial F_p(\hat{\boldsymbol{y}}(k))}{\partial\boldsymbol{u}(k)}+\lambda_e\frac{\partial F_p(\hat{\boldsymbol{e}}(k))}{\partial\boldsymbol{u}(k)},\end{aligned} \tag{28}$$

where $\partial\hat{\boldsymbol{e}}^{\mathrm{T}}(k)/\partial\boldsymbol{u}(k)=\partial\hat{\boldsymbol{y}}^{\mathrm{T}}(k)/\partial\boldsymbol{u}(k)$,

$$\frac{\partial F_p(\hat{\boldsymbol{y}}(k))}{\partial\boldsymbol{u}(k)}=\frac{\partial\hat{\boldsymbol{y}}^{\mathrm{T}}(k))}{\partial\boldsymbol{u}(k)}diag\left(\frac{2s_y sign(\hat{\boldsymbol{y}}(k)-\bar{y})}{y_{\max}-y_{\min}}\right)F_p(\hat{\boldsymbol{y}}(k)), \tag{29}$$

$$\frac{\partial F_p(\boldsymbol{u}(k))}{\partial \boldsymbol{u}(k)} = diag(\frac{2s_u sign(\boldsymbol{u}(k)-\bar{u})}{u_{\max}-u_{\min}})F_p(\boldsymbol{u}(k)), \quad (30)$$

$$\frac{\partial F_p(\hat{\boldsymbol{e}}(k))}{\partial \boldsymbol{u}(k)} = \frac{\partial \hat{\boldsymbol{y}}^{\mathrm{T}}(k))}{\partial \boldsymbol{u}(k)} diag(\frac{2s_e sign(\hat{\boldsymbol{e}}(k)-\bar{e})}{e_{\max}-e_{\min}})F_p(\hat{\boldsymbol{e}}(k)), \quad (31)$$

$$\frac{\partial \Delta \boldsymbol{u}^{\mathrm{T}}(k)}{\partial \boldsymbol{u}(k)} = \begin{bmatrix} 1 & -1 & 0 & \cdots & 0 \\ 0 & 1 & -1 & \cdots & 0 \\ \vdots & \vdots & \vdots & \vdots & \vdots \\ 0 & \cdots & 1 & -1 & 0 \\ 0 & \cdots & 0 & 1 & -1 \end{bmatrix}. \quad (32)$$

The Hessian matrix of the cost function (21) is calculated as

$$\begin{aligned} \frac{\partial^2 \tilde{J}(k)}{\partial \boldsymbol{u}^2(k)} &= 2\frac{\partial \hat{\boldsymbol{e}}^{\mathrm{T}}(k)}{\partial \boldsymbol{u}(k)}\frac{\partial \hat{\boldsymbol{e}}(k)}{\partial \boldsymbol{u}(k)} + 2\rho\frac{\partial \Delta \boldsymbol{u}^{\mathrm{T}}(k)}{\partial \boldsymbol{u}(k)}\frac{\partial \Delta \boldsymbol{u}(k)}{\partial \boldsymbol{u}(k)} \\ &+ \lambda_u \frac{\partial F_p{}^2(\boldsymbol{u}(k))}{\partial \boldsymbol{u}^2(k)} + \lambda_y \frac{\partial F_p{}^2(\hat{\boldsymbol{y}}(k))}{\partial \boldsymbol{u}^2(k)} + \lambda_e \frac{\partial F_p{}^2(\hat{\boldsymbol{e}}(k))}{\partial \boldsymbol{u}^2(k)}, \end{aligned} \quad (33)$$

$$\frac{\partial F_p{}^2(\boldsymbol{u}(k))}{\partial \boldsymbol{u}^2(k)} = diag\left(\frac{(2s_u)^2}{(u_{\max}-u_{\min})^2}F_p(\boldsymbol{u}(k))\right), \quad (34)$$

$$\frac{\partial F_p{}^2(\hat{\boldsymbol{y}}(k))}{\partial \boldsymbol{u}^2(k)} = \frac{\partial^2 \hat{\boldsymbol{y}}^{\mathrm{T}}(k))}{\partial \boldsymbol{u}^2(k)} diag\left(\frac{(2s_y)^2}{(y_{\max}-y_{\min})^2}F_p(\hat{\boldsymbol{y}}(k))\right), \quad (35)$$

$$\frac{\partial F_p{}^2(\hat{\boldsymbol{e}}(k))}{\partial \boldsymbol{u}^2(k)} = \frac{\partial^2 \hat{\boldsymbol{y}}^{\mathrm{T}}(k))}{\partial \boldsymbol{u}^2(k)} diag\left(\frac{(2s_e)^2}{(e_{\max}-e_{\min})^2}F_p(\hat{\boldsymbol{e}}(k))\right). \quad (36)$$

By solving the FHOCP, the optimized control sequence $\boldsymbol{u}^*(k)=[u^*(0|k), u^*(1|k), ..., u^*(N\text{-}1|k)]^{\mathrm{T}}$ is obtained. According to the MPC principle, the first element of the optimal control sequence $u(k)=u^*(0|k)$ is applied to the WWTP system.

3.4 Feasibility and Stability Analysis

In this section, the feasibility of the proposed PC-MPC strategy and the stability of the WWTP system (1) are analyzed. Before moving on, the following assumption is given.

***Assumption* 1:** There exists a terminal control law $u_f(k)$ for system (1), a terminal cost function $\varphi(\hat{e}(N|k))$, a terminal constraint set $\Omega=\{\hat{e}(N|k)\in\mathbb{R}|\varphi(\hat{e}(N|k))\le\iota,\ \iota>0\}$, such that the following conditions hold

1) $\Omega\subseteq Y$;

2) $u_f\in U$ for $y\in\Omega$;

where $\iota\in(0, \infty)$ represents a constant, Y and U represent the set of output and input constraints, respectively.

***Theorem 1*:** For the WWTP system (1) with the control law $u(k)=u^*(0|k)$, the FHOCP is recursively feasible and the WWTP system (1) is asymptotically stable.

***Proof*:** The optimization control sequence of the FHOCP at time k is $\bar{\boldsymbol{u}}^*(k)=[\bar{u}^*(0|k), \bar{u}^*(1|k), ..., \bar{u}^*(N\text{-}1|k)]^{\mathrm{T}}$ satisfying the input constraint (2). Correspondingly, the predicted output sequence at time k is $\hat{\boldsymbol{y}}^*(k)=[\hat{y}^*(1|k), \hat{y}^*(1|k), ..., \hat{y}^*(N|k)]^{\mathrm{T}}$, satisfying the output constraint (3).

The output of system (1) at time k+1 is $y(k+1)$ and a candidate solution is selected as $\boldsymbol{u}(k+1)=[u(0|k+1), u(1|k+1), ..., u(N\text{-}1|k+1)]^{\mathrm{T}}=[u^*(1|k), u^*(2|k), ..., u^*(N\text{-}1|k), u(N\text{-}1|k+1)]^{\mathrm{T}}$. Obviously, the first N-1 elements of $\boldsymbol{u}(k+1)$ are the same as the final N-1 elements of $\boldsymbol{u}^*(t)$, $u(i|k+1)=u^*(i+1|k)$, $i\in[0, N\text{-}2]$, and they all satisfy the input constraint (2). Due to $\hat{y}^*(N|t)\in\Omega$, according to Assumption 1, there can be $u(N\text{-}1|k+1)=u_f(k)\in U$. Thus, the candidate solution satisfies the input constraint (2). The predicted output sequence at time k+1 is $\hat{\boldsymbol{y}}(k+1)=[\hat{y}(1|k+1), \hat{y}(2|k+1), ..., \hat{y}(N|k+1)]^{\mathrm{T}}=[\hat{y}^*(2|k), \hat{y}^*(3|k), ..., \hat{y}^*(N|k), \hat{y}(N|k+1)]^{\mathrm{T}}$. The first N elements of $\hat{\boldsymbol{y}}(k+1)$ satisfy the output constraint (3), $\forall i\in[0, N\text{-}1]$ and form $u_f(k+1)$ have $\hat{y}(N|k+1)\in\Omega$. Therefore, the FHOCP is recursively feasible.

A Lyapunov function is constructed as

$$V(k) = \frac{1}{2}\hat{e}^{\mathrm{T}}(k)\hat{e}(k). \quad (37)$$

The difference of $V(k)$ is calculated as

$$\begin{aligned} \Delta V(k) &= V(k+1) - V(k) \\ &= \Delta\hat{e}^{\mathrm{T}}(k)\hat{e}(k) + \frac{1}{2}\Delta\hat{e}^{\mathrm{T}}(k)\Delta\hat{e}(k), \end{aligned} \quad (38)$$

where $\Delta\hat{e}(k)=\hat{e}(k+1)\text{-}\hat{e}(k)$, calculated as

$$\Delta\hat{e}(k) = \frac{\partial\hat{e}(k)}{\partial u(k)}\Delta u(k) = \Phi\Delta u(k), \quad (39)$$

where $\Phi=\partial\hat{e}(k)/\partial u(k)$.

According to (23), one can get

$$\begin{aligned} \Delta u(k) &= -(\frac{\partial^2\tilde{J}(k)}{\partial u^2(k)} + \mu(k)\mathrm{I})^{-1}\frac{\partial\tilde{J}(k)}{\partial u(k)} \\ &= -(H + \mu(k)\mathrm{I})^{-1}\Phi\hat{e}(t), \end{aligned} \quad (40)$$

where $H=\partial^2\tilde{J}(k)/\partial u^2(k)$.

Substituting (39), (40) into (38), it can be derived

$$\begin{aligned} \Delta V(k) &= \Delta u^{\mathrm{T}}(k)\Phi^{\mathrm{T}}\hat{e}(k) + \frac{1}{2}\Delta u^{\mathrm{T}}(k)\Phi^{\mathrm{T}}\Phi\Delta u(k) \\ &= -\Delta u^{\mathrm{T}}(k)(H + \mu(k)\boldsymbol{I})\Delta u(k) + \frac{1}{2}\Delta u^{\mathrm{T}}(k)\Phi^{\mathrm{T}}\Phi\Delta u(k) \\ &= -\frac{1}{2}\Delta u^{\mathrm{T}}(k)(H + 2\mu(k)\boldsymbol{I})\Delta u(k). \end{aligned} \quad (41)$$

From (41), it can derive $\Delta\hat{V}(k)<0$, then the trajectory of the system (1) is asymptotically stable.

4 Simulation Validation

In this section, the designed PC-MPC strategy and two comparison algorithms: OG-PRWNN [9] and FNN-MPC [19] are applied to the benchmark simulation model No.1 (BSM1) [20] of the activated sludge WWTP to comprehensively evaluate their control performance.

4.1 Simulation Conditions

In this study, the inflow data of BSM1 is sampled from the wastewater treatment plant at a sampling interval of 15 minutes. The constraint for S_{O5} is set to 1.8 mg/L<S_{O5}<2.2 mg/L, and the constraint for K_{La5} was set to 40 day^{-1}<K_{La5}<240 day^{-1}. The performance constraint for tracking error is set to -0.1 mg/L<$e(k)$<0.1 mg/L.

The parameters are selected as: n_y=11, n_u=11, η=0.1, H_y=2, H_u=1, ρ=10^{-6}. The input of the FNN model is $\mathbf{x}(t)=[y(k\text{-}2), ..., y(k\text{-}12), K_{La5}(k\text{-}2), ..., K_{La5}(k\text{-}12)]^{\mathrm{T}}$. To comprehensively evaluate control performance, control strategies are used for fixed set-point tracking and dynamic set-point tracking. The fixed set-point is $y_r(k)$=2 mg/L. The dynamic set-point is set as

$$y_r(k) = \begin{cases} 2.2\text{ mg/L}, & 0\text{ day} < \text{time} < 3.5\text{ day}, \\ 2\text{ mg/L}, & 3.5\text{ day} \le \text{time} < 7\text{ day}, \\ 1.8\text{ mg/L}, & 7\text{ day} \le \text{time} < 10.5\text{ day}, \\ 2\text{ mg/L}, & 10.5\text{ day} \le \text{time} \le 14\text{ day}. \end{cases} \quad (42)$$

The performance evaluation indicators of control strategies are selected as the integral of absolute error (IAE), integral of square error (ISE), and maximum absolute error (DEV^{max})

$$IAE = \frac{1}{M}\sum_{0}^{M}\left|y(k)-y_r(k)\right|, \tag{43}$$

$$ISE = \frac{1}{M}\sum_{0}^{M}\left|y(k)-y_r(k)\right|^2, \tag{44}$$

$$DEV^{max} = \max\left\{\left|y(k)-y_r(k)\right|\right\}, \tag{45}$$

where M represents the sampling number.

4.2 Control Results

The tracking control results of three control methods under the fixed set-point are plotted in Figs. 2-3. Fig. 2 shows the tracking curves and tracking errors of S_{O5} under the fixed set-point. Fig. 3 presents the trend of control input changes during the tracking process of S_{O5} under the fixed set-point. In Fig. 2, the tracking error of the FNN-MPC method is kept in a stable range due to the design of the parameter adaptive mechanism, which can update the parameters of the FNN model according to the prediction error. The tracking error of OG-PRWNN is relatively large at the beginning of the simulation and tends to be stable and kept in a small range after 1 day of learning and training. In contrast, the tracking error of the proposed PC-MPC method can be stably maintained within ± 0.03 mg/L, due to its proper handling of performance constraint. In Fig. 3, for these three methods, the trend of the input signal under the fixed set-point is similar.

The tracking control results of three control methods under the dynamic set-point are plotted in Figs. 4-5. Fig. 4 plots the tracking curves and tracking errors of S_{O5} under the dynamic set-point. Fig. 5 shows the curves of control input for three methods under the dynamic set-point. In Fig.4, the OG-PRWNN method shows higher control accuracy than the FNN-MPC method in the dynamic set-point tracking. This is due to the online growth strategy designed by the OG-PRWNN method, the structure of the controller can be adapted to the system conditions, showing superior learning ability. In contrast, the proposed PC-MPC method not only adapts to different operating conditions but also maintains high tracking accuracy under system constraints. The tracking error of the proposed PC-MPC method remains stable within ± 0.02 mg/L. Fig. 5 illustrates that compared with the OG-PRWNN and FNN-MPC methods, the input signal of the PC-MPC method is relatively stable, which is beneficial for the protection of aeration equipment.

Furthermore, three control strategies are evaluated using IAE, ISE, and DEV^{max} to quantify their accuracy, stability, and response speed. The results of the comparison are outlined in Table 1. Compared with the other two control methods, the minimum IAE (0.0034), ISE (2.6332×10^{-5}), and Dev^{max} (0.0332) are obtained under the fixed set-point tracking, while the minimum IAE (0.0039), ISE (4.1508×10^{-5}), and Dev^{max} (0.0275) are acquired under the dynamic set-point tracking. The comparison results of IAE and ISE indicate that the proposed PC-MPC strategy presents high control accuracy and can accurately follow the set-point. The results of Dev^{max} demonstrate that even under unfavorable conditions, the PC-MPC strategy can maintain small errors.

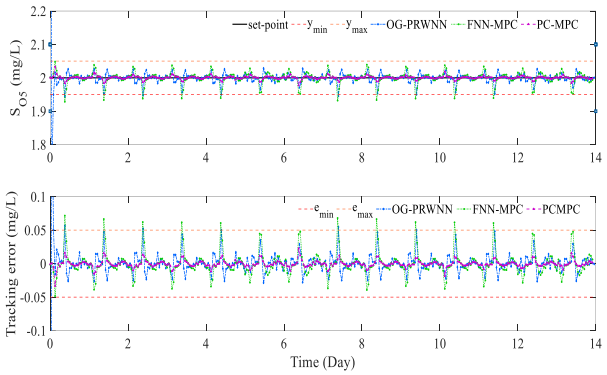

Fig. 2 Tracking results under the fixed set-point.

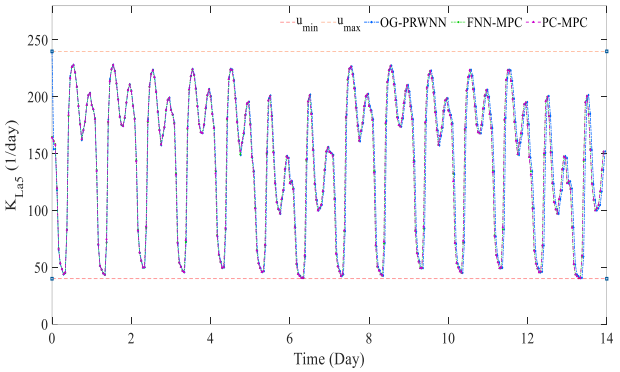

Fig. 3 Control inputs under the fixed set-point.

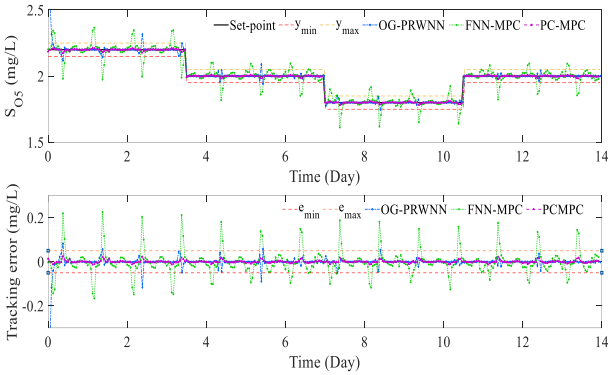

Fig. 4 Tracking results under the dynamic set-point.

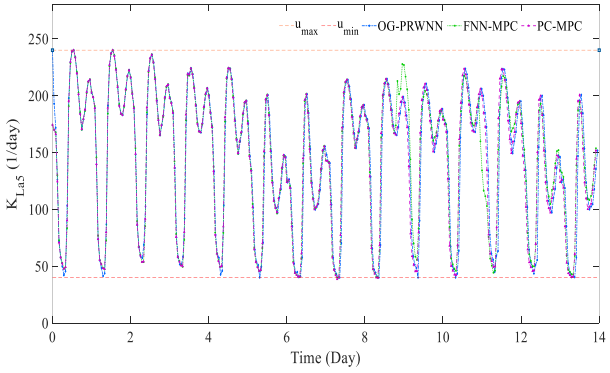

Fig. 5 Control inputs under the dynamic set-point.

Table 1: Comparison results of three control methods

Case	Controller	IAE	ISE	DEV^{max}
fixed set-point	**PC-MPC**	**0.0034**	**2.6332×10^{-5}**	**0.0332**
	FNN-MPC	0.0109	3.1861×10^{-4}	0.0717
	OG-PRWNN	0.0135	0.0058	1.3478
dynamic set-point	**PC-MPC**	**0.0039**	**4.1508×10^{-5}**	**0.0275**
	OG-PRWNN	0.0065	6.9803×10^{-4}	0.4131
	FNN-MPC	0.0335	0.0031	0.2261

5 Conclusion

In this paper, the PC-MPC control strategy was proposed for the accurate control of DO concentration in WWTPs. By constructing a data-driven model based on fuzzy neural network, the difficulty of complex nonlinear identification of wastewater treatment system was addressed, and the prediction error was reduced by combining the model parameter optimization mechanism. On this basis, the MPC strategy with performance constraint was designed to limit the DO concentration tracking error to a predefined acceptable range by dynamically adjusting the control input. Furthermore, a constrained optimization strategy based on L-M algorithm was proposed, which successfully solved the FHOCP problem under multiple constraints and achieved the real-time optimization of the control sequence. The simulation results demonstrated that PC-MPC strategy was superior to the comparison method in both control accuracy and constraint treatment ability, providing theoretical support and technical scheme for the intelligent operation of WWTPs.

References

[1] G. M. Wang, J. Bi, Q. S. Jia, J. F. Qiao, and L. Wang, Event-driven model predictive control with deep learning for wastewater treatment process, *IEEE Trans. Ind. Inf*. 19(5): 6398–6407, 2023.

[2] H. G. Han, Y. S. Wang, Z. Liu, H. Y. Sun, and J. F. Qiao, Knowledge-data driven optimal control for nonlinear systems and its application to wastewater treatment process, *IEEE Trans. Cybern.*, 54(10): 6132–6144, 2024.

[3] H. G. Han, C. C. Feng, H. Y. Sun, and J. F. Qiao, Self-organizing fuzzy terminal sliding mode control for wastewater treatment processes, *IEEE Trans. Autom. Sci. Eng*. 21(4): 5421–5433, 2024.

[4] P. Zhou, X. A. Wang, and T. Y. Chai, Multiobjective operation optimization of wastewater treatment process based on reinforcement self-learning and knowledge guidance, *IEEE Trans. Cybern.*, 53(11): 6896–6909, 2023.

[5] H. G. Han, Y. Q. Xing, and H. Y. Sun, Adaptive robust fuzzy sliding mode control for wastewater treatment processes, *IEEE Trans. Fuzzy Syst*., 32(8): 4787–4798, 2024.

[6] P. H. Du, W. M. Zhong, X. Peng, L. L. Li, and Z. Li, Self-healing control for wastewater treatment process based on variable-gain state observer, *IEEE Trans. Ind. Inf*. 19(10): 10412–10424, 2023.

[7] H. G. Han, Y. M. Xu, Z. Liu, H. Y. Sun, J. F. Qiao, Knowledge-data-driven robust fault-tolerant control for sludge bulking in wastewater treatment process, *IEEE Trans. Ind. Inf*. 20 (8): 10280–10291, 2024.

[8] H. G. Han, S. J. Fu, H. Y. Sun, and C. Y. Wang, Robust model free adaptive predictive control for wastewater treatment process with packet dropouts, *IEEE Trans. Cybern.*, 54(10): 6069–6080, 2024.

[9] J. F. Qiao, Y. Su, and C. L. Yang, Online-Growing neural network control for dissolved oxygen concentration, *IEEE Trans. Ind. Inf*., 19(5): 6794–6803, 2023.

[10] K. Stebel, J. Pospiech, W. Nocon, J. Czeczot, and P. Skupin, Boundary-based predictive controller and its application to control of dissolved oxygen concentration in activated sludge bioreactor, *IEEE Trans. Ind. Electron*., 69(10): 10541–10551, 2022.

[11] P. Hang, X. Xia, G. Chen, and X. B. Chen, Active safety control of automated electric vehicles at driving limits: A tube-based MPC approach, *IEEE Trans. Transp. Electrif*., 8(1): 1338–1349, 2022.

[12] D. P. Li, H. G. Han, and J. F. Qiao, Fuzzy-approximation adaptive fault tolerant control for nonlinear constraint systems with actuator and sensor faults, *IEEE Trans. Fuzzy Syst*., 32(5): 2614–2624, 2024.

[13] R. Q. Chai, A. Tsourdos, H. J. Gao, Y. Q. Xia, and S. C. Chai, Dual-loop tube-based robust model predictive attitude tracking control for spacecraft with system constraints and additive disturbances, *IEEE Trans. Ind. Electron.*, 69(4): 4022–4033, 2022.

[14] P. Zhou, X. Y. Sun and T. Y. Chai, Enhanced NMPC for stochastic dynamic systems driven by control error compensation with entropy optimization, *IEEE Trans. Control Syst. Technol.*, 31(5): 2217–2230, 2023.

[15] H. G. Han, S. J. Fu, H. Y. Sun, and J. F. Qiao, Data-driven model-predictive control for nonlinear systems with stochastic sampling interval, *IEEE Trans. Syst. Man Cybern.: Syst*., 53(5): 3019–3030, 2023.

[16] Y. Xu, S. Li, W. Zhang, G. Yu, and J. Zou, Long-horizon constrained model predictive direct speed control for PMSM drives based on Laguerre functions, *IEEE Trans. Control Syst. Technol*., 32(3): 1002–1014, 2024.

[17] S. Yan, P. J. Goulart, and M. Cannon, Stochastic MPC with dynamic feedback gain selection and discounted probabilistic constraints, *IEEE Trans. Autom. Control*, 67(11): 5885–5899, 2022.

[18] C. C. Feng, H. Y. Sun, H. G. Han, Z. Cheng, and F. Y. Li, Robust dynamic surface control with fixed time observer for wastewater treatment processes, in *2024 43rd Chinese Control Conference (CCC)*, 2024: 2227–2232.

[19] H. G. Han, Z. Liu, J. F. Qiao, Fuzzy neural network-based model predictive control for dissolved oxygen concentration of WWTPs, *Int. J. Fuzzy Syst*. 21 (5), 1497–1510, 2019.

[20] A. Khurshid, A. K. Pani, Machine learning approaches for data-driven process monitoring of biological wastewater treatment plant: A review of research works on benchmark simulation model No. 1(BSM1), *Environ. Monit. Assess*. 195 (8), 1–19, 2023.